ЖУРНАЛ СТРУКТУРНОЙ ХИМИИ

2017. Том 58, № 2 *Февраль – март* *С. 261 – 268*

UDC 541.6:547.12

TAUTOMERISM OF THE ANTIEPILEPTIC DRUG FELBAMATE: A DFT STUDY

A. Khaleghi-Rad, S.A. Beyramabadi, A. Morsali, M. Ebrahimi, M. Khorasandi-Chenarboo

Department of Chemistry, Mashhad Branch, Islamic Azad University, Mashhad, Iran
E-mail: beyramabadi@yahoo.com

Received June, 27, 2015 *Revised — November, 15, 2015*

The Felbamate is a novel anticonvulsant and neuropathic pain drug that can exist as three possible tautomers. Herein, employing density functional theory (DFT) and handling the solvent effects with the PCM model, the structural parameters, energy behavior, natural bond orbital analysis (NBO), as well as the tautomerism of Felbamate are investigated. **F1** is the kinetically and thermodynamically most stable tautomer of Felbamate, which contains the amide group in each of the carbamate moieties. The calculated NMR chemical shifts and IR vibrational frequencies are in good agreement with the experimental values, confirming the suitability of the optimized geometry for Felbamate. The tautomerization reaction of **F1** to each of the other tautomers occurs via an intramolecular proton transfer. This reaction affects considerably the structural parameters and atomic charges of the Felbamate molecule. A large HOMO-LUMO energy gap implies a high stability of the **F1** tautomer.

DOI: 10.15372/JSC20170204

K e y w o r d s: Felbamate, Taloxa, DFT, PCM, tautomerism, intramolecular proton transfer.

INTRODUCTION

Felbamate (FBM, Taloxa) or 2-phenyl-1,3-propanediol dicarbamate is a new antiepileptic drug that was marketed under the brand name Felbatol by MedPointe_in 1993. Alone or in combination with other medications, Felbamate is used to treat seizures in adults and children with epilepsy. This drug cuts off or minimizes the number of seizures. Felbamate is effective in treatment of the Lennox—Gastaut syndrome in children, too [1—7]. Felbamate is a dicarbamate that involves a phenyl group at the 2-carbon position. This drug is readily absorbed from the gastrointestinal tract. It is only slightly soluble in water and increasingly soluble in ethanol, methanol, and DMSO [8, 9].

Nowadays, DFT is widely employed in many areas of computational chemistry, such as geometry optimizations, spectroscopic assignments, investigations of the reaction kinetics and mechanisms, drug science, and so on [10—14].

The knowledge of the structural and spectroscopic properties of drugs is an essential prerequisite for understanding their biological activity. So far, no crystal structure has been reported for Felbamate and no theoretical study has been published on this compound. Therefore, a detailed theoretical investigation on Felbamate is of major importance. In this work, we address this issue and examine its molecular geometry, tautomerism, vibrational frequencies, NMR chemical shifts, and the natural bond orbital (NBO) analysis using valuable DFT approaches.

THEORETICAL

All of the present calculations have been performed with the Gaussian 03 software package [15] using the B3LYP [16] functional and the 6-311+G(*d*,*p*) basis set. For the investigation of solvent ef-

fects in an aqueous solution, one of the self-consistent reaction field methods, the sophisticated polarized continuum model (PCM) [17] has been employed.

First, all geometries were fully optimized. The optimized geometries were confirmed to have no imaginary frequency, except for the transition state (TS) that has only one imaginary frequency of the Hessian. The zero-point corrections and thermal corrections have been considered in evaluation of the energies. The optimized geometry was used to compute the vibrational frequencies, NMR chemical shifts, atomic charges, and the NBO analysis.

The ^{1}H NMR chemical shifts were obtained with respect to tetramethylsilane, where the GIAO method was used [18]. Since the DFT calculated vibrational frequencies are usually higher than the experimental ones, they were scaled using a factor of 0.9614 [19]. All structures were visualized using the Chemcraft 1.7 program [20].

RESULTS AND DISCUSSION

Molecular geometry. The Felbamate drug can exist as three possible tautomers whose geometries have been fully optimized in the gas phase and an aqueous solution in the PCM model. Their PCM optimized geometries are shown in Fig. 1. For each tautomer, we have employed only the most stable conformer.

Felbamate is a dicarbamate drug. As seen in Fig. 1, the **F1** tautomer has an amide group (—CO(NH_2)) in each of the carbamate moieties. In comparison with **F1**, in the **F2** tautomer the H3 proton is transferred from the N1 atom of the —NH_2 group to the O4 carbonyl oxygen atom via an intermolecular proton transfer (IPT). In **F3**, both H1 and H3 protons of two amine groups are transferred to the oxygen atoms of the carbonyl groups, O3 and O4, respectively. Important structural parameters of the optimized geometries are gathered in Table 1.

The relative energies of the three tautomers are gathered in Table 2, where the zero-point corrections have been considered. As seen, **F1** is the most stable tautomer of Felbamate in both gas and solution phases.

Tautomerization mechanism. F1 is the most stable tautomer of Felbamate, which can be converted to **F2** and finally to **F3** *via* IPT. Herein, the tautomerism of Felbamate was investigated using DFT methods.

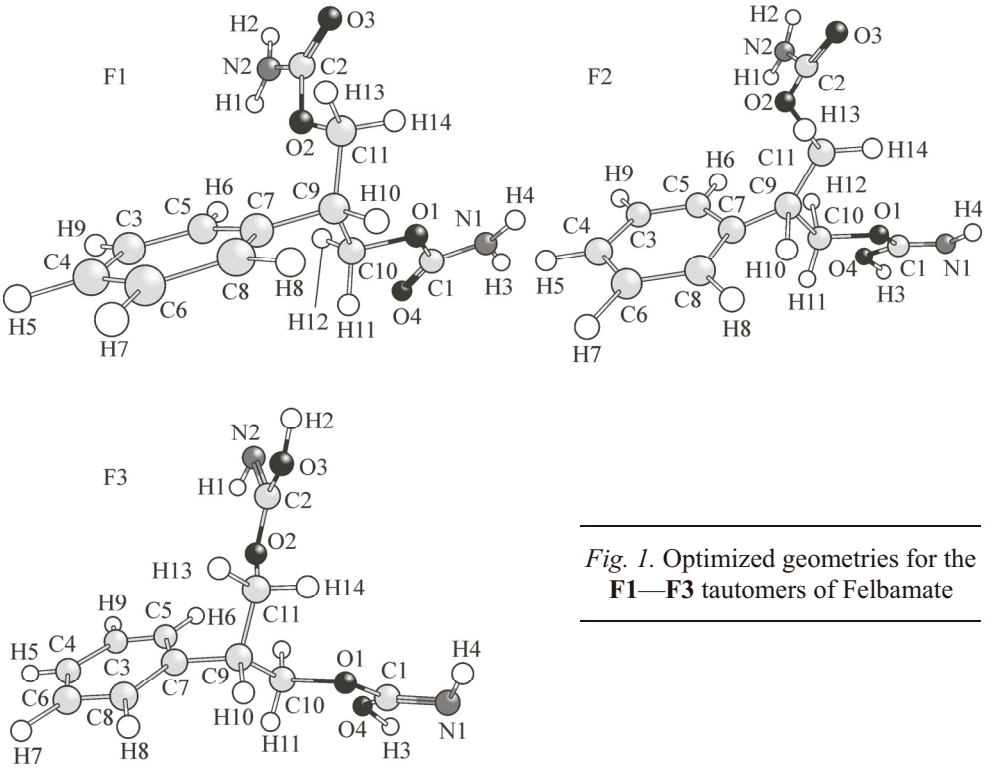

Fig. 1. Optimized geometries for the **F1**—**F3** tautomers of Felbamate

Table 1

Selected structural parameters for the optimized geometries

Parameters	**F1**	**F2**	**F3**	**TSF1-F2**	**TSF2-F3**
Bond length, Å					
N1—H3	1.00	2.32	2.32	1.34	1.34
O4—H3	2.54	0.96	0.96	1.29	1.29
N2—H2	1.00	1.00	2.31	1.00	1.00
C2—N2	1.35	1.35	1.27	1.35	1.35
C1—O4	1.22	1.34	1.34	1.29	1.29
C1—O1	1.35	1.33	1.33	1.31	1.31
Angle, deg.					
H3—N1—C1	118.2	54.03	54.01	72.27	72.27
N1—C1—O4	125.2	122.1	122.2	107.7	107.7
N1—C1—O1	110.7	124.5	124.4	127.2	127.2
O4—C1—O1	124.0	113.3	113.2	124.9	124.9
C1—O1—C10	116.5	120.2	120.2	117.6	117.6
H1—N2—H2	118.6	118.6	164.6	118.6	118.6
C2—O2—C11	116.5	116.5	120.2	116.5	116.5
Dihedral angle, deg.					
H1—N2—H2—O3	–165.8	–165.9	179.97	–166.3	–166.3
N2—C2—O2—C11	–178.7	–178.7	179.6	–178.8	–178.8
O3—C2—O2—C11	0.004	–0.01	–0.35	–0.01	–0.014
C2—O2—C11—C9	177.6	177.8	179.0	176.9	177.9
C11—C9—C10—O1	58.92	59.14	59.44	59.32	59.32
C10—O1—C1—N1	178.2	179.6	179.6	–179.4	–179.4
C10—O1—C1—O4	–0.608	–0.47	–0.44	0.507	0.50
O4—C1—N1—H3	–10.02	0.094	0.107	0.066	0.06
C11—C9—C7—C8	–108.1	–108.3	–106.0	–108.3	–108.3
C9—C7—C8—C6	179.9	179.9	179.7	179.8	179.8
C4—C6—C7—C5	0.036	0.040	0.041	0.037	0.037

TS of the **F1→F2** tautomerization was called **TSF1-F2**. The optimized geometry for **TSF1-F2** is shown in Fig. 2, in which the cleavage of the N1—H3 bond together with the formation of the O4—H3 bond is clear.

Going from **F1** to the **F2** tautomer, some structural parameters have changed, the most important changes being: N1—H3…O4 and O4—H3…N1 H-bond lengths are 2.54 and 1.00 Å in the F1 tautomer, respectively, which change to 0.96 and 2.32 Å in the **F2** one. These parameters are 1.29 and 1.34 Å in **TSF1-F2**. The C1—N1 bond length decreases from 1.35 to 1.27 Å, whereas the C1—O4 bond length enlarges from 1.22 to 1.34 Å. These bond lengths are 1.30 and 1.29 Å in **TSF1-F2**.

Table 2

Relative energies ($kJ \cdot mol^{-1}$) *of the* **F1**—**F3** *tautomers of Felbamate*

Species	Gas phase	PCM model	Species	Gas phase	PCM model
F1	0.0	0.0	**TSF1-F2**	207.22	216.26
F2	88.76	93.04	**TSF2-F3**	295.18	309.37
F3	175.89	186.14			

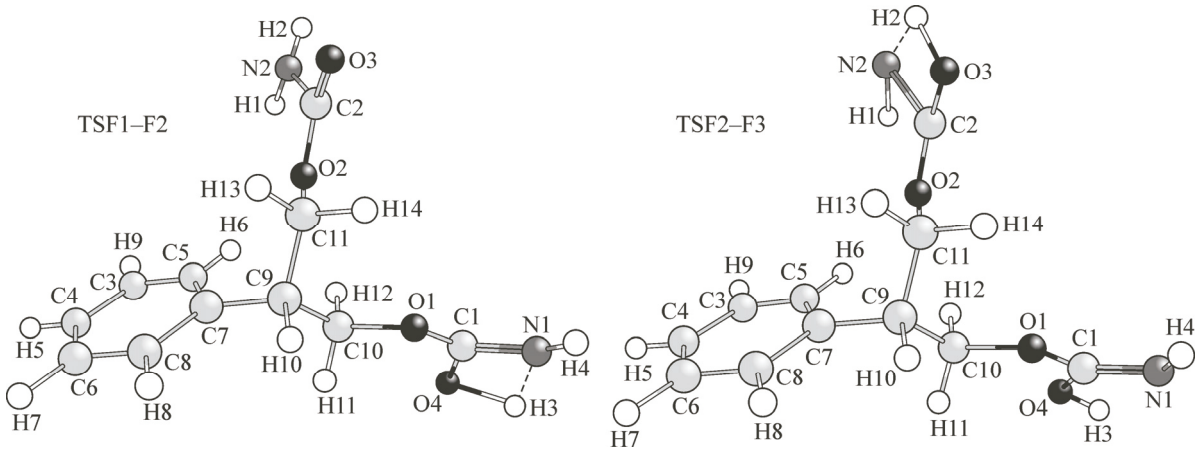

Fig. 2. Optimized geometries for **TSF1-F2** and **TSF2-F3**

TSF2-F3 is optimized TS for the **F2→F3** tautomerization, whose optimized geometry is shown in Fig. 2. As seen, the cleavage of the N2—H2 bond is obvious as well as the formation of the O3—H2 bond.

Important changes in the structural parameters during the **F2→F3** tautomerization are: N2—H2…O3 and O3—H2….N2 H-bond lengths are 2.54 and 1.00 Å in the **F2** tautomer, respectively, which change to 0.96 and 2.31 Å in the **F3** one. These parameters are 1.29 and 1.34 Å in **TSF2-F3**. The C2—N2 bond length decreases from 1.35 to 1.27 Å, whereas the C2—O3 bond length enlarges from 1.22 to 1.34 Å. These bond lengths are 1.30 and 1.29 Å in **TSF2-F3**.

Considering the equilibrium between the **F1**, **F2**, **F3** tautomers, the value of the tautomeric equilibrium constant (K) is calculated using

$$K = \exp\left(-\frac{\Delta G}{RT}\right), \tag{1}$$

where ΔG, R, and T are the Gibbs free energy difference between the three tautomers, the gas constant, and the temperature, respectively. In the solution phase, the Gibbs free energy difference between the most stable tautomer **F1** with the **F2** and **F3** tautomers are 90.57 kJ·mol^{-1} and 178.08 kJ·mol^{-1}, respectively. By Eq. (1), the amounts of the **F2** and **F3** tautomers in an aqueous solution of Felbamate are predicted to be negligible.

IR and NMR spectra. Nowadays, the theoretical analysis of the spectra is employed as a valuable tool for the identification of chemical compounds [10—14]. Herein, the IR and NMR spectra of the most stable tautomer of Felbamate (**F1**) were assigned theoretically using DFT methods.

The vibrational modes of **F1** were analyzed by comparing the DFT and experimental IR spectra. Assignments of the selected vibrational frequencies are gathered in Table 3. Some weak to medium bands in the 3500—3000 cm^{-1} spectral region of Felbamate can be related to the overlap of the N—H and C—H stretching vibrations [11—13, 21, 22]. The deconvolution of this region is given in Table 3. The most intense band is related to the symmetric stretching vibrations of the amine group. Also, a very strong band at 1691 cm^{-1} is attributed to the stretching modes of the carbonyl moieties.

For comparison, the experimental ^{1}H NMR chemical shifts (δ) of Felbamate together with the computational values for the **F1** tautomer are gathered in Table 4. The atomic positions are numbered as in Fig. 1.

As seen, the DFT calculated chemical shifts and vibrational frequencies are in good agreement with the experimental values, confirming the suitability of the optimized geometry for **F1** as the most stable tautomer of Felbamate.

NBO analysis. The NBO analysis is a useful tool for the investigation of the intra- and intermolecular bonding interactions and charge transfer in chemical compounds [13, 25]. The NBO atomic charges of all optimized geometries are selectively listed in Table 5. The computed charges indicate a

Table 3

Selected experimental and calculated IR *vibrational frequencies* (cm^{-1}) *of the* **F1** *tautomer*

Experimental[a]	Calculated		Vibrational assignment
	Wavenumbers	Intensity ($kJ \cdot mol^{-1}$)	
703 (s)	685	89	δ(benzene ring)
765 (m)	750	33	δ(amide group)
1064 (s)	1029	300	υ(C1—O1, C2—O2)
	1070	108	
1082 (s)	1102	25	υ_{asym}(C10—C9—C11)
1138 (m)	1271	519	υ_{sym}(N1—C1—O1, N2—C2—O2)
1348 (m)	1283	665	
1614 (s)	1544	165	δ_{sci}(NH_2 group)
1691 (vs)	1660	554	υ(C1—O4, C2—O3)
300—3500	2926	12	υ(C9—H10)
	2950	63	υ_{sym}(CH_2)
	2997, 3001	34, 27	υ_{asym}(CH_2)
	3038—3074	10, 34	υ(C—H) aromatic
	3462	125	υ_{sym}(NH_2)
	3581	105	υ_{asym}(NH_2)

[a] The experimental results were obtained from [23].

Table 4

Experimental and theoretical ^{1}H NMR *chemical shifts of Felbamate and its* **F1** *tautomer in the* DMSO *solution* δ (ppm)

Atomic position	Theor.	Exp.[a]
H10	3.12	3.1
H11	3.83	6.4
H13	3.96	
H14	4.48	
H12	4.55	
H5, H8	7.53	7.2
H7, H9	7.69	
H6	7.77	

[a] The experimental results were obtained from [24].

Table 5

Atomic natural charges of the investigated species

Atom	NBO atomic charges				
	F1	**TSF1-F2**	**F2**	**TSF2-F3**	**F3**
C7	–0.03	–0.04	–0.03	–0.04	–0.04
C9	–0.27	–0.28	–0.27	–0.28	–0.27
H10	0.22	0.22	0.22	0.23	0.22
C10	–0.02	–0.02	–0.02	–0.02	–0.02
O1	–0.59	–0.54	–0.58	–0.58	–0.58
C1	0.91	0.88	0.85	0.85	0.85
O4	–0.65	–0.72	–0.70	–0.70	–0.70
N1	–0.82	–0.88	–0.78	–0.78	–0.78
H3	0.40	0.50	0.50	0.50	0.50
H4	0.40	0.39	0.35	0.35	0.35
C11	–0.01	–0.02	–0.02	–0.02	–0.02
O2	–0.59	–0.60	–0.60	–0.55	–0.58
C2	0.91	0.91	0.91	0.88	0.85
O3	–0.65	–0.65	–0.65	–0.72	–0.70
N2	–0.82	–0.82	–0.82	–0.88	–0.78
H1	0.40	0.40	0.40	0.39	0.35
H2	0.40	0.40	0.40	0.50	0.50

T a b l e 6

Second order perturbation theory analysis of the Fock matrix in the NBO *basis for the* **F1** *tautomer of Felbamate*

Donor NBO (*i*)	Acceptor NBO (*j*)	$E_j - E_i$, a.u. [a]	$E(2)$, kJ·mol [b]
BD(2) C3—C5	BD*(2) C4—C6	0.28	84.35
BD(2) C3—C5	BD*(2) C7—C8	0.28	88.70
BD(2) C4—C6	BD*(2) C3—C5	0.28	85.02
BD(2) C4—C6	BD*(2) C7—C8	0.28	83.77
BD(2) C7—C8	BD*(2) C3—C5	0.28	82.30
BD(2) C7—C8	BD*(2) C4—C6	0.28	86.40
LP(1) O1	BD*(1) C1—O4	0.88	20.61
LP(1) O1	BD*(2) C1—O4	0.87	21.07
LP(2) O1	BD*(1) C1—O4	0.64	47.61
LP(2) O1	BD*(2) C1—O4	0.63	49.12
LP(2) O1	BD*(1) C10—H11	0.73	20.65
LP(2) O1	BD*(1) C10—H12	0.73	17.97
LP(1) O2	BD*(1) C2—O3	0.89	21.11
LP(1) O2	BD*(2) C2—O3	0.86	20.48
LP(2) O2	BD*(1) C2—O3	0.65	45.52
LP(2) O2	BD*(2) C2—O3	0.62	51.62
LP(2) O2	BD*(1) C11—H13	0.73	18.60
LP(2) O2	BD*(1) C11—H14	0.73	19.98
LP(2) O3	BD*(1) C2—O2	0.61	127.91
LP(2) O3	BD*(1) C2—N2	0.7	89.91
LP(2) O4	BD*(1) C1—O1	0.61	128.16
LP(2) O4	BD*(1) C1—N1	0.7	89.83
LP(1) N1	BD*(1) C1—O4	0.59	63.16
LP(1) N1	BD*(2) C1—O4	0.58	55.30
LP(1) N2	BD*(1) C2—O3	0.6	60.44
LP(1) N2	BD*(2) C2—O3	0.57	57.68

[a] Energy difference between the donor (*i*) and acceptor (*j*) NBO orbitals.

[b] Energy of hyperconjugative interactions.

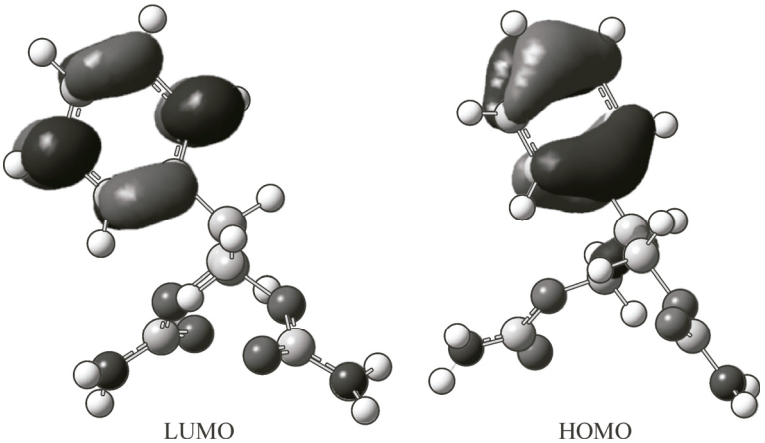

Fig. 3. HOMO and LUMO frontier orbitals of the **F1** tautomer

high positive charge on the H3 and H2 atoms during the **F1**—**F2** and **F2**—**F3** tautomerization, respectively, displaying IPT between the donor nitrogen atoms and acceptor oxygen atoms. As expected, in **F1**→**F2** and **F2**→**F3** IPTs, the negative charge of the donor oxygen atoms increases, whereas that of the acceptor nitrogen atoms decreases.

Electron delocalization between the donor NBO(i) and acceptor NBO(j) orbitals results in the stabilization energy of hyperconjugative interactions (E(2)). The E(2) amount is a criterion for determining the degree of interaction between the electron donor and acceptor orbitals. The greater the E(2), the greater the electron transferring tendency from the electron donor to the electron acceptor, causing higher electron density delocalization, and consequently, more stabilizing the system. The E(2) value is calculated using [13, 26]

$$E(2) = -q_i \frac{(F_{ij})^2}{\varepsilon_j - \varepsilon_i}, \quad (2)$$

where q_i, F_{ij}, ε_j, and ε_i parameters are the donor orbital occupancy, the off-diagonal NBO Fock matrix element, the energies of the acceptor and donor orbitals, respectively. The lower $\varepsilon_j - \varepsilon_i$ energy difference leads to higher E(2) stabilization energy. The parameters of Eq. (2) have been obtained from the second order perturbation theory analysis of the Fock matrix in the NBO basis. The selected results for the most stable tautomer of Felbamate (**F1**) are gathered in Table 6.

As seen, the strongest interactions inducing the highest stabilization energies are related to the LP(O3) → σ*(C2—O2) and LP(O4) → σ*(C1—O1) electron donations. There are weak electron donations from n(O1) to the σ* orbital of the C10—H11 and C10—H12 bonds, and from n(O2) to the σ* orbital of the C11—H13 and C11—H14 bonds, too. These NBO interactions imply the existence of weak C10—H…O1 and C11—H…O2 hydrogen bond interactions by about 20 kJ/mol as the stabilizing energy.

The 3D distribution map for the highest occupied molecular orbital (HOMO) and the lowest unoccupied molecular orbital (LUMO) of the **F1** tautomer are shown in Fig. 3. Both HOMO and LUMO orbitals are localized on the benzene ring. As seen in the first rows of Table 6, the $\pi \rightarrow \pi^*$ transitions of the benzene ring stabilize the molecule.

The energy difference between the frontier HOMO and LUMO orbitals is one of the important characteristics of molecules, which plays a determining role in electric properties, electronic spectra, and photochemical reactions. The energy gap between the HOMO and LUMO orbitals of the **F1** tautomer is 6.41 eV. This large energy gap demonstrates that the structure of Felbamate is very stable [27, 28].

CONCLUSIONS

Felbamate is a new antiepileptic drug. Herein, the optimized geometries and energy characteristics of three possible tautomers of Felbamate, as well as the kinetics and mechanism of its tautomerization have been theoretically studied in detail using DFT methods.

F1 is the most stable tautomer of Felbamate, which involves two amide groups at both sides of the molecule. This tautomer can be converted to the **F2** and **F3** tautomers via IPT. The computed atomic charges support IPT during the tautomerization. Both **F1**⇄**F2** and **F1**⇄**F3** tautomerism reactions have a roughly high energy barrier. Therefore, **F1** is the most kinetically and thermodynamically favorable tautomer of Felbamate. There is also good consistency between the DFT predicted and experimentally-reported chemical shifts and vibrational frequencies, confirming the validity of the optimized geometry for **F1** as the most stable tautomer of Felbamate.

The HOMO and LUMO frontier orbitals of **F1** are localized on the benzene ring. A large HOMO-LUMO energy gap was obtained, indicating a high stability of this tautomer.

REFERENCES

1. *Hansen R.J., Samber B.J., Gustafson D.L.* // J. Chromatogr. B. – 2010. – **878**. – P. 3432.
2. *Heyman E., Levin N., Lahat E., Epstein O., Gandelman-Marton R.* // Eur. J. Paediatr. Neurol. – 2014. – **18**. – P. 658.
3. *Brown W.M., Aiken S.P.* // Crit. Rev. Neurobiol. – 1998. – **12**. – P. 205.
4. *Palmer K., McTavish D.* // Drugs. – 1993. – **45**. – P. 1041.
5. *Pellock J.M., Faught E., Leppik I.E., Shinnar S., Zupanc M.L.* // Epilepsy Res. – 2006. – **71**. – P. 89.
6. *Sofia R.D.* // Ann. Neurol. – 1994. – **36**. – P. 677.
7. *Zupanc M.L., Roell Werner R., Schwabe M.S., O'Connor S.E., Marcuccilli C.J., Hecox K.E., Chico M.S., Eggener K.A.* // Pediatr. Neurol. – 2010. – **42**. –P. 396.
8. *Rho M.J., Donevan S.D., Rogawski M.A.* // J. Pharmacol. Exp. Ther. – 1997. – **280**. – P. 1383.
9. *Patsalos P.N., Berry D.J., Bourgeois B.F.D., Cloyd J.C., Glauser T.A., Johannessen S.I., Leppik I.E., Tomson T., Perucca E.* // Epilepsia. – 2008. – **49**. – P. 1239.
10. *Galasso V.* // Chem. Phys. Lett. – 2009. – **472**. – P. 237.
11. *Eshtiagh-Hosseini H., Beyramabadi S.A., Morsali A., Mirzaei M., Chegini H., Elahi M., Naseri M.A.* // J. Mol. Struct. – 2014. – **1072**. – P. 187.
12. *Beyramabadi S.A., Morsali A., Javan-Khoshkholgh M., Esmaeili A.A.* // J. Struct. Chem. – 2012. – **53**. – P. 460.
13. *Sadeghzade Z., Beyramabadi S.A., Morsali A.* // Spectrochim. Acta, Part A. – 2015. – **138**. – P. 637.
14. *Beyramabadi S.A., Morsali A., Vahidi S.H., Javan Khoshkholgh M., Esmaeili A.A.* // J. Struct. Chem. – 2012. – **53**. – P. 665.
15. *Frisch M.J. et al.* // Gaussian 03, Revision B.03. – Gaussian Inc.: Pittsburgh PA, 2003.
16. *Lee C., Yang W., Parr R.G.* // Phys. Rev. B. – 1988. – **37**. – P. 785.
17. *Tomasi J., Cammi R.* // J. Comput. Chem. – 1995. – **16**. – P. 1449.
18. *Ditchfield R.* // Mol. Phys. – 1974. – **27**. – P. 789.
19. *Young D.C.* Computational Chemistry: A Practical Guide for Applying Techniques to Real-World Problems. – John Wiley & Sons, 2001.
20. *Zhurko G.A., Zhurko D.A.* Chemcraft 1.7. http://www.chemcraftprog.com.
21. *Sanmartín J., García-Deibe A.M., Fondo M., Navarro D., Bermejo M.R.* // Polyhedron. – 2004. – **23**. – P. 963.
22. *Ware D.C., Mackie D.S., Brothers P.J., Denny W.A.* // Polyhedron. – 1995. – **14**. – P. 1641.
23. *Sparagana S.P., Strand W.R., Adams R.C.* // Epilepsia. – 2001. – **42**. – P. 682.
24. *Thompson C.D., Barthen M.T., Hopper D.W., Miller T.A., Quigg M., Hudspeth C., Montouris G., Marsh L., Perhach J.L., Sofia R.D., Macdonald T.L.* // Epilepsia. – 1999. – **40**. – P. 769.
25. *Snehalatha M., Ravikumar C., Hubert Joe I., Sekar N., Jayakumar V.S.* // Spectrochim. Acta, Part A. – 2009. – **72**. – P. 654.
26. *Schwenke D.W., Truhlar D.G.* // J. Chem. Phys. – 1985. – **82**. – P. 2418.
27. *Tezer N., Karakus N.* // J. Mol. Model. – 2009. – **15**. – P. 223.
28. *Özdemir N., Dinçer M., Çukurovah A., Büyükgüngör O.* // J. Mol. Model. – 2009. – **15**. – P. 1435.